

1 Electron microscopic reconstruction of functionally identified cells
2 in a neural integrator.

3 Ashwin Vishwanathan,¹* Kayvon Daie,³ Alejandro D. Ramirez,³
Jeff W Lichtman,⁴ Emre Aksay,³ and H. Sebastian Seung^{1,2}

¹Neuroscience Institute and ²Computer Science Department
Princeton University, Princeton, NJ 08544

³Institute for Computational Biomedicine and
Department of Physiology and Biophysics,

Weill Cornell Medical College, New York, NY 10021

⁴Department of Molecular and Cellular Biology and Center for Brain Science,
Harvard University, Cambridge, MA 02138

4 February 14, 2017

5 **Abstract**

6 Neural integrators are involved in a variety of sensorimotor and cognitive behaviors. The oculomotor system con-
7 tains a simple example, a hindbrain neural circuit that takes velocity signals as inputs, and temporally integrates them
8 to control eye position. We combined observations of behavior, physiology, and anatomy to study integrator neurons.
9 Two-photon calcium imaging of the larval zebrafish hindbrain was performed while simultaneously monitoring spon-
10 taneous eye movements, followed by serial electron microscopy. Integrator neurons were identified as those neurons
11 with activities highly correlated with eye position, and the same neurons were then reconstructed from serial electron
12 microscopic images. Three morphological classes of neurons were observed: ipsilaterally projecting neurons located
13 medially, contralaterally projecting neurons located more laterally and a population at the extreme lateral edge of the
14 hindbrain for which we were not able to identify axons. Based on their somatic locations, we infer that neurons with
15 only ipsilaterally projecting axons are glutamatergic, whereas neurons with only contralaterally projecting axons are
16 largely GABAergic. Dendritic and synaptic organization of the ipsilaterally projecting neurons suggest a broad sam-
17 pling from inputs on the ipsilateral side. We also observe the first conclusive evidence of synapses between integrator
18 neurons, which have long been hypothesized by recurrent network models of integration via positive feedback.

19 **1 Introduction**

20 Combining two-photon calcium imaging with serial electron microscopy (EM) is an emerging approach for studying
21 the structure and function of neural circuits at cellular resolution. In the mouse retina [1] and primary visual cortex
22 [2, 3], this approach has been used to study the structure and function of visual neurons. Here we apply this approach
23 to a population of neurons defined by their encoding of behavioral variables, rather than stimulus variables. Namely,
24 we focus on neurons that carry eye position signals that are located in a hindbrain neural circuit known as the "velocity-
25 to-position neural integrator," or "neural integrator" for short [4, 5]. Our study is done in the larval zebrafish, which
26 has emerged as an important model organism for investigating the relation between neural circuits and behavior [6].

27 The neural integrator gets its name because the transformation of eye velocity into eye position is the computational
28 operation of integration with respect to time. Integrator neurons are operationally defined as premotor neurons that
29 carry a horizontal eye position signal in their spiking (there is also an integrator for vertical eye movements, but it
30 will not be discussed here). Integrator neurons are thought to send their eye position signals to extraocular motor

*Corresponding author

31 neurons through monosynaptic and polysynaptic pathways. They are also thought to receive inputs from multiple
32 convergent pathways that encode eye velocity for every type of eye movement. Therefore, the neural integrator is the
33 “final common pathway” for all types of eye movements in fish [7, 8, 9], rodents [10], non-human primates [11, 12],
34 and humans [13].

35 Previous attempts to understand how the integrator neurons transforms eye velocity signals to eye position signals
36 have relied on combining single-neuron electrophysiology with light-microscopic dye fills. Intracellular recordings in
37 goldfish hindbrain neurons that exhibited spiking correlated to eye position, followed by anatomical dye fills, show the
38 axons of these neurons send collaterals to areas where other integrator neurons were observed [8]. Similar anatomical
39 observations have been observed in cats [14] and nonhuman primates [15]. These observations have shaped theoretical
40 models to propose that integration can be setup by recurrent excitation between these neurons [16, 17, 18, 19, 20].
41 More recent imaging methods have relied on two-photon calcium imaging to identify many integrator neurons followed
42 by sparse, targeted single neuron electroporation of fluorescent indicators for anatomical reconstruction [21]. While
43 these studies have delineated the arborization and projection patterns of integrator neurons, they were limited to one
44 or a few neurons in any individual brain and do not reveal locations and the distributions of their input and output
45 synapses. And although the axonal projections could potentially synapse onto dendrites of other integrator neurons,
46 conclusive evidence has been lacking.

47 We combined two-photon calcium imaging and serial electron microscopy to identify neurons in the neural in-
48 tegrator and reconstruct the same neurons. We found evidence for multiple classes of neurons within the integrator
49 population based on differences in dendritic arborization, axonal projections and synaptic distributions. These include
50 neurons with ipsilaterally projecting axons at medial locations that are inferred to be excitatory, and neurons with con-
51 trilaterally projecting axons at more caudal locations that are inferred to be inhibitory. In addition, we found neurons
52 at the lateral most edge of the volume, for which we could not identify an axon, and a previously unreported integrator
53 neuron with both ipsilateral and contralateral axonal projections. We identified all chemical synapses in our images
54 by the existence of presynaptic vesicles and postsynaptic densities. Chemical synapses involving integrator neurons
55 contained small vesicles, suggesting the presence of conventional rather than peptidergic neurotransmitters. Finally
56 we report evidence for direct synaptic connectivity between integrator neurons.

57 2 Results

58 2.1 Combined two-photon and electron microscopy of integrator neurons

59 To identify putative integrator neurons we performed two-photon calcium imaging of the caudal hindbrain in a 6 dpf
60 larval zebrafish following bolus loading of the calcium sensor Oregon Green BAPTA 1-AM. The functional imaging
61 was restricted to one side where the loading was best and was performed on three planes that were ~8 μm apart during
62 spontaneous eye movement. Calcium signals were correlated with eye position to identify integrator somata from
63 the imaged planes (Fig. 1A) [22]. Neurons were identified as integrator neurons if saccade-triggered eye position
64 following an ipsiversive saccade (Fig. 1A,b arrow) was correlated with saccade-triggered average fluorescence (Fig.
65 1A,c first column) (Pearson coefficient > 0.6). The integration time constants or the level of persistence was quantified
66 as the time constant of an exponential fit to the firing rate profile determined from a deconvolution of the fluorescence
67 data (Fig. 1A, c, dotted line, extend methods). This resulted in the identification of 22 integrator neurons from 3
68 distinct imaging planes with graded levels of persistence (Sup Fig. 1A, B).

69 Following functional identification of integrator neurons, the tissue was optically imaged (LM), fixed, stained,
70 sectioned for serial electron microscopy and imaged at a final resolution of 5 × 5 × 45 nm (RC, ML, DV). These
71 images were montaged and aligned to create a 3D electron microscopy volume (EM) (Fig. 1B and Methods). The
72 resulting EM volume extended ventrally from the Mauthner cell axon plane by ~60 μm , caudally from the border of
73 rhombomere 5/6 by ~200 μm and laterally from the midline by ~100 μm . The LM and EM volumes were registered
74 to each other by an affine transform, producing correspondence of labeled neurons and blood vessels (Fig. 1C, Sup.
75 Fig. 1C, Methods). The soma of all 22 integrator neurons from the LM volume were located in the EM volume within
76 the rhombomeres 6,7 and 8 (Fig 1D, colored by time constants).

77 2.2 Stripe shaped patterning of somata in the hindbrain

78 Cell bodies in the hindbrain of the larval zebrafish follow a stereotypic stripe like pattern of alternating cell bodies and
79 neuropil. Cells within the same stripe typically share the same neurotransmitter identity, and morphology [23, 24, 25].

80 To extract this stripe like organization, we projected the locations of all cell somata (Fig. 1D, 'o' symbol) from the
81 high-resolution imaged area onto a single plane. The high-res EM volume contained a total of 2967 somata spread
82 over rhombomeres 5 through 8 (Fig. 1D). The volume also contained well-known landmarks like the Mauthner
83 neuron [26], the axon of the contralateral Mauthner neuron, neurons MiD2 and MiD3 of the reticulo-spinal network
84 [26], and a number of commissural bundles (Fig. 1D). This procedure revealed an alternating pattern of cell somata
85 and neuropil. We were able to locate 3 peaks of cell somata, excluding a peak that corresponds to neurons at the
86 midline, each corresponding to a likely stripe (Fig. 1D, bottom panel, S1-3). The three stripes were labeled based
87 on their proximity to the midline, as medial (S1), intermediate (S2) and lateral stripe (S3) respectively. **The medial**
88 **most stripe S1 aligns with a group of neurons that express the *alx* transcription factor, that also expresses glutamate.**
89 **More dorsally, this stripe is laterally abutted by cells that express the *engrailed -1* transcription factor which expresses**
90 **glycine** [27, 24], but previous work has show that at this depth (below the level of the Mauthner axon) the vast majority
91 **of integrator neurons are glutamatergic and not glycinergic** [21]. The intermediate stripe S2 corresponds to neurons
92 known to express the transcription factor *dbx1b* [24]. The majority of integrator neurons in this stripe express GABA,
93 while a small minority express glutamate. At the ventral locations explored here, integrator neurons in this stripe are
94 almost exclusively GABAergic [21]. The lateral most peak S3 of neurons corresponds with the expression of the *barhl*
95 transcription factor, which is also thought to be glutamatergic [28, 24].

96 **2.3 Anatomical properties of integrator neurons**

97 After the identification of the integrator neurons in the EM volume, we reconstructed all 22 integrator neurons and
98 annotated the pre- and postsynaptic locations for these neurons (extended methods). We first characterized some of
99 the anatomical properties that were common to all integrator neurons.

100 **Somata**

101 The somatic locations of the 22 integrator neurons were distributed over ~23 μm in the dorsoventral axis and along
102 the entire rostrocaudal extent of the imaged volume. A subset of these neurons were located very close to the midline
103 and at the rostral edge of the imaged volume, close to the border of rhombomeres 6,7 and at the caudal end of the
104 imaged volume, located in rhombomere 8, roughly between myotomes 1, 2. Another subset of neurons was located
105 at the lateral end of the volume in rhombomere 8. The diameters of the integrator neurons were normally distributed,
106 with a mean of $4.5 \pm 0.6 \mu\text{m}$ (mean \pm standard deviation). In general, the size of the somata was proportional to the
107 persistence level of the neurons, with larger neurons exhibiting higher degree of persistence (Sup. Fig. 1B (right),
108 Pearson coefficient = 0.4, $p= 0.059$). On average 3.3 ± 1.5 neurites emerged from the somata, and traveled ventrally.

109 **Synapses**

110 We annotated 320 presynaptic (green circles, Fig. 2) and 2195 postsynaptic sites (red circles, Fig. 2) on the 22 integrator
111 neurons. Synapses were identified by the presence of a presynaptic vesicle pool and an opposing postsynaptic
112 density. Synapses from or onto integrator neurons contained small vesicles, presumably containing a conventional
113 neurotransmitter. Elsewhere in the volume we did identify synapses with dense core vesicles, presumably containing
114 a peptide neurotransmitter (Sup. Fig. 2A).

- 115 • Integrator presynaptic sites

116 The presynaptic site was generally at a varicosity in the axon with vesicles throughout. Opposing the postsynaptic
117 density, a small, denser cluster of vesicles was typically observed, along with the presynaptic density. These features
118 are consistent with the idea of a presynaptic active zone. The number of presynaptic sites on a neuron averaged
119 62.3 ± 39.2 . This is an underestimate of the number of output synapses from an integrator neuron, because most
120 axonal arbors were cut off by the borders of the volume. If statistics are restricted to the 3 neurons that were more
121 complete than others, there were 84 ± 48.5 presynaptic sites.

- 122 • Integrator postsynaptic sites

123 The postsynaptic densities were observed as a darkening of the membrane, indicative of more electron dense regions,
124 corresponding to more protein density. The number of postsynaptic sites on a neuron averaged 99.7 ± 72.4 . This is
125 a reasonable estimate of the number of input synapses to an integrator neuron, because most dendritic arbors were
126 reconstructed in their entirety.

127 • Cell Junctions

128 Along the somatic membrane, a darkening of the membrane interrupted by small gaps was often observed (Sup. Fig.
129 2B). The darkening persisted over multiple serial sections, suggesting that it was not an artifact of tissue preparation or
130 imaging. These darkenings were visible between somata of integrator-integrator and integrator-non-integrator neurons.
131 We speculate that these darkenings are some kind of cell junction. Else where it has been noted that gap junctions
132 exist in the developing larval zebrafish hindbrain [29].

133 **Dendrites**

134 Dendrites were defined by the absence of presynaptic vesicles and the presence of postsynaptic densities. They were
135 mostly oriented ventral to the location of the somata. Dendrites were smooth rather than spiny. Some dendrites
136 exited the imaged volume, leading to incompletely reconstructed neurons. **Neurons with small dendritic arbors were**
137 **completely reconstructed and did not have any dendrites that exited the imaged volume.**

138 **Axons**

139 We defined axons as neurites with a) presynaptic vesicles or b) for cases where there were no presynaptic vesicles,
140 define them as putative axons using additional anatomical cues (addressed below). Regions of transition, from dendrite
141 to axon, we termed axon initiation sites. Example axon initiation sites are indicated in Fig. 2, showing the dendrite
142 (neurite with red postsynaptic sites) turning into axons at the axon initiation (open arrow). The main trunk of the
143 axon extended rostrally and ventrally (Fig. 2 A, B). From the main trunk emerged mediolateral branches, which we
144 will term collaterals. Those at the rostral extreme of the volume appeared to overlap with the expected location of the
145 abducens motor nucleus (based on its known position within rhombomere r5, 6 Sup. Fig. 3A), with terminations in
146 r4 as well.

147 We observed sheaths around some axonal segments. In some locations, we saw that the sheath wrapped around
148 the axon a few times, loosely enough that cytoplasmic space was visible (Fig. 2A, EM panel). This was consistent
149 with the definition of loose myelin [30]. This is different from the more conventionally observed compact myelin
150 which appears as dark as seen elsewhere in the volume. The axon of the neuron in Fig. 2A was intermittently
151 loosely myelinated along its rostrocaudal section. Mediolateral collaterals emerged from the gaps in loose myelin, and
152 remained unmyelinated. Such loose myelin sheaths have been previously reported in goldfish [31].

153 In 10/22 (45%) integrator neurons the presence of a contralaterally projecting putative axon was identified. Be-
154 cause neurites in the contralateral hindbrain were not reconstructed, we relied on several other features for axon
155 determination. First the putative axons were devoid of any postsynaptic sites on the ipsilateral side (Fig. 2 B, D open
156 arrow to end, no synapses). The lack of postsynaptic sites on these putative axons is similar to the initial segment of
157 conventional axons that were identified by the presence of vesicles, where no presynaptic terminals in the proximal
158 part of the axon were observed, and presynaptic sites emerged only distally (Fig. 2B, initial segment of axon). Sec-
159 ondly, before crossing the midline, the putative axon became engulfed by processes that appeared glial in nature (Fig.
160 2 C, D, EM inset G). The glial engulfment is consistent with the idea of ‘glial bridges’ that are instrumental in the
161 guidance of axons during development [32]. Thirdly, these putative axons were thinner than the remaining neurites of
162 the neuron. The diameter of these putative axons were smaller to the other neurites and were similar to the diameters of
163 conventional axons (Sup. Fig. 1E). The mean axonal diameter was less than the mean dendrite diameter, conforming
164 to the textbook notion that axons are thinner than dendrites. These features were applied to determine a neurite to be
165 a putative axon.

166 **Small protuberances**

167 A small fraction (~4% or 91/2195) of the postsynaptic sites were located on finger-like projections from dendrites that
168 were enveloped by invaginations of axonal boutons (Fig. 2B, EM panel 2). These projections resemble structures
169 found across multiple species called *spinules*, and are thought to be present on large, active synapses [33].

170 We also observed a primary cilium on all 22 integrator neurons. Primary cilium are known to be present in most, if
171 not all mammalian cells, including neurons, and are thought to be important for normal development [34]. The average
172 cilium was typically ~ 4 μ m, is enriched with microtubules, and emerges from the neuron somata very close to the
173 Golgi complex. In some cases, this primary cilium terminated inside processes that resembled glial like structures

¹⁷⁴ (Sup. Fig. 4A). Orientation of primary cilium in integrator neurons did not show any orientation preference (Sup. Fig.
¹⁷⁵ 4B).

¹⁷⁶ 3 Axonal projection patterns of integrator neurons

¹⁷⁷ The reconstructed integrator neurons were then divided into three groups based on the spatial projection patterns of
¹⁷⁸ the axons that were identified. Below we have detailed the properties of integrator neurons from each of these groups.

¹⁷⁹ Ipsilateral projection only (“ipsi-only”) - Six neurons located at the rostral edge of the volume, were observed
¹⁸⁰ to have only ipsilaterally projecting axons (Fig. 3A). Two representatives are shown in Figs. 2A and B. The axons
¹⁸¹ were clearly identified by the presence of *en passant* boutons with presynaptic vesicles. The somata were located at the
¹⁸² rostral extent of the volume, close to the midline (Fig. 3A, Ipsi. only). The axons were oriented along the rostro-caudal
¹⁸³ (RC) axis with the rostral end more ventral as compared to the caudal end. The average length of axons was $\sim 260\mu\text{m}$
¹⁸⁴ (Sup. Table) with the longest reconstructed axon being $463\mu\text{m}$. Two of the six axons had projections that terminate
¹⁸⁵ near the site of the abducens motor nuclei (Sup. Fig. 4B). The axon initiation site was on average located $\sim 99\mu\text{m}$
¹⁸⁶ from the somata. Finally, none of the axons were observed emerging directly from the somata. Instead, dendrites
¹⁸⁷ bearing postsynaptic sites turned into axons with presynaptic sites.

¹⁸⁸ Neurons in this group had large dendritic arbors, with the dendrites arborizing over 22.5% of the total imaged
¹⁸⁹ volume (Sup. Fig. 5A, B, C). The dendrites emerged laterally from somata and always extended ventrally. Only in
¹⁹⁰ one case the dendrites were observed to cross the midline, as indicated by the presence of postsynaptic sites (Fig. 3A,
¹⁹¹ Ipsi. only, arrowheads). The average diameter of dendrites was significantly larger as compared to the diameter of the
¹⁹² axons (Fig. 3F, $p < 2 \times 10^{-3}$, ttest).

¹⁹³ Contralateral projection only (“contra-only”) - Nine neurons located at the caudal end of the imaged volume
¹⁹⁴ contained exclusively contralaterally projecting putative axons (Fig. 3A, Contra only). Like the axons in the ipsi-only
¹⁹⁵ group, the putative contralateral axons did not emerge as axons, but started as a neurite with postsynaptic sites, that
¹⁹⁶ became axonal. However, unlike the ipsi-only group, the axon initiation site was much closer to the somata. On
¹⁹⁷ average, the axon initiation site was located $\sim 22\mu\text{m}$ from the somata, which is significantly shorter than the axon
¹⁹⁸ initiation site for the ipsi-only group ($p < 0.0003$, ttest).

¹⁹⁹ The average dendritic length was $\sim 290\mu\text{m}$, and the dendritic arbors of these neurons arborized over 8% of the total
²⁰⁰ volume (Sup. Fig. 5A, B, C). This was significantly smaller than the dendritic arbors of ipsi-only group, ipsi-contra
²⁰¹ group combined ($p < 0.003$, ttest). The average diameter of dendrites significantly larger than the diameter of the
²⁰² axons (Fig. 3F, $p < 2 \times 10^{-6}$, ttest). The diameter of dendrites of the contra-only neurons was significantly smaller to
²⁰³ the ipsi-only group (Fig. 3F, $p < 0.005$, ttest).

²⁰⁴ Projection unknown (“unknown”) - Seven neurons were located at the lateral most extent of the animal. For these
²⁰⁵ neurons we did not find any neurites with presynaptic sites nor could we locate a putative axon (Fig. 3A, Unknown).
²⁰⁶ We believe this is most likely because these neurons were not fully represented in the imaged volume and neurites of
²⁰⁷ these neurons exit the volume before the axon was located. The average length of the dendrites for neurons from this
²⁰⁸ group was $\sim 220\mu\text{m}$, and they occupied on average $\sim 4.9\%$ of the total volume (Sup. Fig. 5A, B, C).

²⁰⁹ Finally one integrator neuron did not fit into any of these three groups, its axon had both an ipsilateral and contralat-
²¹⁰ eral projection (Supp. methods, Sup. Fig. 5A).

²¹¹ 3.1 Organization of integrator neuron synapses

²¹² Neurons from these three groups had on average, 170, , 84 and 40 postsynaptic (inputs) sites on their dendrites
²¹³ respectively (Fig. 3B, red). The axons from the ipsi-only groups had approximately 58 presynaptic (output) sites
²¹⁴ (Fig. 3B, green). The pathlength of each synaptic location from the somata revealed that the distribution of the
²¹⁵ postsynaptic sites along the dendrites among the Ipsi and Contra, unknown groups were significantly different (Fig.
²¹⁶ 3D, $p = 7.2 \times 10^{-13}$, $p = 1.2 \times 10^{-10}$ kstest).

²¹⁷ We further computed the synaptic density, the number of synapses per unit length for all neurons, with the assump-
²¹⁸ tion that the synapses within each group were uniformly distributed along dendrites. The uniformity assumption was
²¹⁹ made because the distributions of the locations of postsynapses was found to closely match the location of dendritic
²²⁰ arbors (Sup. Fig. 6A). We found the there were $\sim 1.5 \times$ more input synapses on the ipsi-only group of neurons, as
²²¹ compared to the inputs on the contra-only group of neurons (ipsi-only group median number 0.42 inputs per mi-
²²² cron, contra-only group 0.26 input per micron, Fig. 3C, $p = 0.049$, Wilcoxon-rank test). Empirically the average

223 intersynaptic distance for the ipsi-only and contra-only groups of neurons are $1 \pm 2.3\mu m$ and $1.2 \pm 1.6\mu m$ (Fig. 3E,
224 $p = 1.2 \times 10^{-10}$ Wilcoxon-rank test).

225 **3.2 Planar organization of dendrites**

226 The dendrites of the neurons from the ipsi-only and contra-only groups were observed to lie along orthogonal planes.
227 The dendrites of the neurons in the ipsi-only group were noticed to lie roughly along a coronal plane with some tilt (Fig.
228 3A). Similarly, the dendrites of the neurons in the contra neurons were noticed to exhibit some planar organization as
229 well. Fitting a plane through the postsynaptic sites that lie along the dendrites of the neurons in these groups revealed
230 that these planes were nearly orthogonal (82.4°) to each other (Fig. 4A).

231 The dendritic arbors of the neurons in these two groups displayed an inversion in the stratification depths. The
232 dendritic arbors of the ipsi-only neurons on average were most abundant at $38.1 \pm 8.2\mu m$ ventral to its somata (Fig.
233 4B, top). Whereas the contra-only group was maximal around $12.2 \pm 8.2\mu m$ ventral to its somata (Fig. 4B, bottom).
234 Interestingly, when we overlaid the stripe patterns computed previously (Fig. 1D) with the stratification profiles of the
235 dendrites along the medio-lateral axis, we see that the dendrites and axons of the ipsi-only group projected arbors that
236 overlapped with neurons along the S1 and S3 stripes , whereas the dendrites of the contra group were located very
237 close the intermediate S2 stripe. Similar loose organization was observed for the other group of neurons (Sup. Fig.
238 6B).

239 **3.3 Connectivity between integrator neurons**

240 We also examined the patterns of connectivity between integrator neurons. We found that there exists varying amounts
241 of overlap of the axons of the ipsilaterally projecting neurons (Sup. Fig. 6C) with the dendrites of all other neurons
242 in the volume. More specifically, the overlap at ventro-rostral locations were from axons of ipsi-only neurons onto
243 dendrites of other ipsi-only neurons (Sup. Fig. 6C, D Ipsi->Contra). Whereas, the overlap at dorso-caudal locations
244 were from axons of ipsi-only neurons onto dendrites of contra-only and unknown group of neurons (Sup. Fig. 6C, D).

245 Furthermore, we found 6 synapses between integrator neurons. Two synapses made by one ipsi-only neuron onto
246 another, and 4 synapses onto three contra-only neurons (Fig. 4C).

247 **4 Discussion**

248 We combined two-photon calcium imaging from neurons in the larval zebrafish that were encoding for a behavioral
249 variable (eye-position) with serial section electron microscopy. This was done by registering the light microscopic
250 volume to the electron microscopic volume to locate the same neurons. We were able to reconstruct 22 integrator
251 neurons from the same animal, for which we had both functional and structural information. This procedure revealed
252 the existence of distinct groups of neurons that make up the ipsilateral integrator circuit. This included an excitatory,
253 ipsilaterally projecting group, an inhibitory, contralaterally projecting group and, a third, excitatory group with
254 unknown projections. Finally we provide the first conclusive evidence for synapses between integrator neurons.

255 Of the 22 integrator neurons, six, rostrally located neurons had exclusively ipsilaterally projecting axons. All
256 but one of these six neurons were medial to the first somata stripe S1, that is thought to contain mostly excitatory,
257 glutamatergic neurons. The axons and dendrites of these neurons display a planar organization, with axons oriented
258 approximately orthogonal to the dendrites (Sup. Fig. 6D). The majority of input synapses onto the dendrites of these
259 neurons lie along a plane approximately normal to the rostro-caudal (RC) axis. This suggests that these neurons are
260 setup to broadly sample from axons that are oriented along the RC axis. The axons of these neurons are oriented
261 along the RC axis with the rostral end more ventral than the caudal end. This suggests that axons from this group
262 can potentially synapse onto dendrites from this group. It has long been theorized that positive feedback via recurrent
263 excitation could be a possible mechanism that can explain long persistent time scales of neuronal activity [18, 19, 35].
264 Indeed, we observed conclusive chemical synapses from one ipsilaterally projecting integrator neuron onto another
265 ipsilaterally projecting integrator neuron. These facts point to the ipsi group of neurons as a candidate that could
266 support recurrent positive feedback in the integrator circuit.

267 The second major group of neurons that we reconstructed were the nine caudally located, contralaterally projecting
268 neurons. The somatic location of these neurons lie very close to the intermediate somal stripe S2, that are largely
269 GABAergic neurons. The dendrites of these neurons arborized over a smaller area, and stratify more dorsally as

270 compared to the ipsi-only group of neurons. The postsynaptic inputs on the dendrites of these cells lie along a plane
271 that is approximately parallel to the RC plane. This suggests that these neurons sample narrowly from inputs along
272 the RC axis. In the goldfish oculomotor integrator, contralaterally projecting neurons are thought to be involved in
273 coordinating activity between the two sides, where each side acts as an independent integrator [36, 37]. Although, we
274 have not reconstructed the contralateral side of the axons, evidence from light microscopic images of contralaterally
275 projecting neurons shows projections that terminate in the dendritic field of the opposing population of inhibitory
276 integrator neurons [21].

277 Of the remaining integrator neurons, one had both an ipsilateral and contralaterally projecting axon. The location
278 of its somata corresponded with the S2 stripe, which can be inferred as GABAergic. The remaining integrator neurons
279 were located at the lateral edge of the animal corresponding to the lateral most stripe S3 and are thought to express
280 glutamate. Since these neurons are close to the edge of the imaged volume, in all cases, we were unable to trace many
281 neurites from these cells. The axonal projection pattern and potential role of these neurons remains unknown.

282 Our evidence suggest that at least two of the groups, the ipsilaterally projecting and the contralaterally projecting
283 neurons are unique populations. They have significantly different dendritic morphologies, axonal projections and
284 distributions of postsynapses along their dendrites. The ipsi-only group of neurons has approximately twice as many
285 postsynaptic input sites as the contra-only only group. In both cases initiation of the axons was from a neurite that
286 contained postsynaptic sites that then gave rise to presynaptic sites. This feature could be important to influence
287 the activity of neurons as these locations are proximal to the somata. Finally we note that distinguishing axons from
288 dendrites using light microscopy can prove erroneous, since the diameters of the axons and dendrites were very similar
289 and close to the diffraction limit of light.

290 Our sample of 22 reconstructed integrator neurons is a fraction of the roughly 100 integrator neurons estimated
291 to exist on one side of the larval zebrafish brain [38]. We observed 6 chemical synapses from two ipsilaterally pro-
292 jecting integrator neurons onto other integrator neurons. This observation may be an underestimate of integrator
293 connectivity, for a few reasons. First, there are many neurons in the imaged volume that carried no usable calcium
294 signal at all, largely because they did not take up enough calcium indicator. Some of these neurons are likely to be
295 integrator neurons overlooked by our study, and are potential postsynaptic partners of the reconstructed neurons in
296 our sample. Second, there are integrator neurons outside the imaged volume, and they could receive synapses from
297 our reconstructed integrator neurons. Only three axonal arbors were fully or mostly reconstructed; the rest appeared
298 substantially cut off as their axons left the volume, this is also evidenced by the fact that only two of six ipsilaterally
299 projecting axons project to the abducens motor nuclei, contrary to dye fill experiments, where all ipsilateral axons
300 project to the abducens. Third, we had no possibility of finding connections between neurons on opposite sides of the
301 brain, because only one side of the brain was imaged. Therefore, it is difficult to know whether the two neurons that
302 made synapses onto other integrator neurons are an exceptional case, or representative of a larger population that was
303 incompletely sampled. More definitive information about connectivity patterns between integrator neurons awaits a
304 future experiment with an imaged volume that is large enough to encompass all integrator neurons, and a fluorescent
305 calcium indicator that labels a higher percentage of integrator neurons.

306 Here we presented ultrastructural anatomical details of different types of integrator neurons and evidence of synap-
307 tic connectivity between these neurons. Although we restricted our reconstructions to the unilateral integrator circuit
308 and consequently do not know about the postsynaptic targets of the contralaterally projecting axons, this approach can
309 be used to uncover general rules of connectivity and validate hypothesized theories of temporal integration.

310 5 Experimental procedures and Methods

311 Light and electron microscopic imaging

312 Anesthetized *nacre* mutant zebrafish larvae was imaged with calcium sensitive dye Oregon Green 488 BAPTA-
313 1 AM. Following functional imaging, the animal was imaged on the same setup for anatomical imaging with x,y
314 resolution of $0.53\mu m$ and z of $1.33\mu m$. The tissue was stained using a reduced osmium staining procedure [39].
315 Following staining, the tissue was infiltrated with an LX-112 based resin. Serial sections from the above animal
316 were collected approximately from the level of the Mauthner neuron at a thickness of 45 nm. The serial sections
317 were collected using the automatic tape-collecting ultramicrotome (ATUM) [40, 41]. Each wafer was imaged in a
318 Zeiss Sigma field emitting scanning electron microscope in the backscattered electron mode using a custom software
319 interface to collected the images [40]. For the high-resolution each section was imaged at a lateral resolution of
320 5nm/pixel in a region of interest that roughly corresponded with the area imaged on the light microscopic. The EM

321 volume we imaged contained 15791 image tiles (8000×8000 pixels each) or $\sim 10^{11}$ pixels. The imaged volume was
322 $220 \times 112 \times 57 \mu\text{m}^3$.

323 Registration of light microscope and electron microscope volumes

324 Following the functional imaging, the animal was re-imaged at higher axial resolution of $1 \mu\text{m}$ between optical
325 planes. This imaging made visible anatomical landmarks like blood vessels and location of neuron bodies, this volume
326 was termed the light microscopy (LM) volume. These landmarks served as fiducial marks to register the EM and LM
327 volume using the TrakEM2 plugin in Fiji [42]. This let us extract the locations of neurons whose firing had high degree
328 of correlation to eye-position, and had the firing characteristic of neural integrator neurons, similar to [22, 43, 44].

329 These images were registered using the TrakEM2 plugin in Fiji [42]. Briefly, individual images were first montaged
330 using affine transforms followed by elastic transforms. Following this they were aligned in the z dimension, using first,
331 affine and followed by elastic transforms.

332 **6 Author contributions**

333 Conceptualization, Methodology, and Writing: A.V, E. A., and H.S.S. Formal Analysis: A.V. and H.S.S. Data Cura-
334 tion: A.V. Visualization: A.V. Investigation: K.D performed two-photon calcium imaging. A.V. acquired serial section
335 EM images with assistance from J.W.L., and assembled the resulting image stack. K.D, A.R. registered the calcium
336 images with the EM images. A.V. and E. A. reconstructed neurons with help from A.R. Funding Acquisition: E.A.
337 and H.S.S.

338 **7 Acknowledgments**

339 We are grateful to Juan Carlos Tapia, Richard Schalek and Ken Hayworth for assisting us with tissue preparation, the
340 ATUM serial sectioning procedure, and the WaferMapper software for EM imaging. Stefan Saalfeld, Albert Cardona,
341 and Ignacio Arganda-Carreras answered questions about the TrakEM2 plugin for FIJI/ImageJ. Uygar Sümbül assisted
342 with importing skeletons into MATLAB. We thank Heather Sullivan for tissue processing and optimization, Ashleigh
343 Showler, Gurion Marks and Anjin Xianyu for assistance with reconstructions and alignment. We benefited from
344 helpful discussions with David Tank and Kanaka Rajan. HSS acknowledges funding from the Mathers Foundation,
345 Gatsby Foundation, Human Frontier Science Program, NIH/NINDS award 5R01NS076467, and ARO MURI award
346 W911NF-12-1-0594.

347 References

- 348 [1] Kevin L Briggman, Moritz Helmstaedter, and Winfried Denk. Wiring specificity in the direction-selectivity
349 circuit of the retina. *Nature*, 471(7337):183–188, March 2011.
- 350 [2] Davi D Bock, Wei-Chung Allen Lee, Aaron M Kerlin, Mark L Andermann, Greg Hood, Arthur W Wetzel, Sergey
351 Yurgenson, Edward R Soucy, Hyon Suk Kim, and R Clay Reid. Network anatomy and in vivo physiology of
352 visual cortical neurons. *Nature*, 471(7337):177–182, March 2011.
- 353 [3] WCA Lee, V Bonin, M Reed, B J Graham, and G Hood. Anatomy and function of an excitatory network in the
354 visual cortex. *Nature*, 2016.
- 355 [4] Guy Major and David Tank. Persistent neural activity: prevalence and mechanisms. *Current opinion in neurobiology*,
356 14(6):675–684, December 2004.
- 357 [5] M Joshua and S G Lisberger. A tale of two species: Neural integration in zebrafish and monkeys. *Neuroscience*,
358 296:80–91, June 2015.
- 359 [6] Rainer W Friedrich, Gilad A Jacobson, and Peixin Zhu. Circuit Neuroscience in Zebrafish. *Current Biology*,
360 20(8):R371–R381, April 2010.
- 361 [7] A M Pastor, R R De la Cruz, and R Baker. Eye position and eye velocity integrators reside in separate brainstem
362 nuclei. *Proceedings of the National Academy of Sciences*, 91(2):807–811, January 1994.
- 363 [8] E Aksay, R Baker, H S Seung, and D W Tank. Anatomy and Discharge Properties of Pre-Motor Neurons in the
364 Goldfish Medulla That Have Eye-Position Signals During Fixations. *Journal of Neurophysiology*, 84(2):1035–
365 1049, August 2000.
- 366 [9] E Aksay, G Gamkrelidze, H S Seung, R Baker, and D W Tank. In vivo intracellular recording and perturbation
367 of persistent activity in a neural integrator. *Nature neuroscience*, 4(2):184–193, February 2001.
- 368 [10] A M van Alphen, J S Stahl, and C I De Zeeuw. The dynamic characteristics of the mouse horizontal vestibulo-
369 ocular and optokinetic response. *Brain research*, 890(2):296–305, February 2001.
- 370 [11] D A Robinson. Integrating with neurons. *Annual review of neuroscience*, 1989.
- 371 [12] Freda Newcombe. Neuropsychology quainterface. *Journal of Clinical and Experimental Neuropsychology*,
372 7(6):663–681, January 2008.
- 373 [13] R John Leigh and David S Zee. *The Neurology of Eye Movements*. Oxford University Press, USA, June 2015.
- 374 [14] R A McCrea and R Baker. Cytology and intrinsic organization of the perihypoglossal nuclei in the cat. *The
375 Journal of comparative neurology*, 237(3):360–376, July 1985.
- 376 [15] H J Steiger and J A Büttner-Ennever. Oculomotor nucleus afferents in the monkey demonstrated with horseradish
377 peroxidase. *Brain research*, 160(1):1–15, January 1979.
- 378 [16] B Yeshwant Kamath and Edward L Keller. A neurological integrator for the oculomotor control system. *Mathematical Biosciences*, 30(3-4):341–352, January 1976.
- 380 [17] H S Seung. How the brain keeps the eyes still. *Proc. Natl. Acad. Sci. USA*, 93(23):13339–13344, 1996.
- 381 [18] H Sebastian Seung, Daniel D Lee, Ben Y Reis, and David W Tank. Stability of the Memory of Eye Position in a
382 Recurrent Network of Conductance-Based Model Neurons. *Neuron*, 26(1):259–271, April 2000.
- 383 [19] D Fisher, I Olasagasti, D W Tank, E R F Aksay, and M S Goldman. A modeling framework for deriving the
384 structural and functional architecture of a short-term memory microcircuit. *Neuron*, 79(5):987–1000, 2013.
- 385 [20] P J Gonçalves, A B Arrenberg, B Hablitzel, H Baier, and C K Machens. Optogenetic perturbations reveal the
386 dynamics of an oculomotor integrator. *Frontiers in Neural Circuits*, 8, 2014.

- 387 [21] Melanie M Lee, Aristides B Arrenberg, and Emre R F Aksay. A Structural and Genotypic Scaffold Underlying
388 Temporal Integration. *The journal of neuroscience*, 35(20):7903–7920, May 2015.
- 389 [22] Andrew Miri, Kayvon Daie, Rebecca D Burdine, Emre Aksay, and David W Tank. Regression-Based Iden-
390 tification of Behavior-Encoding Neurons During Large-Scale Optical Imaging of Neural Activity at Cellular
391 Resolution. *Journal of Neurophysiology*, 105(2):964–980, February 2011.
- 392 [23] Shin-Ichi Higashijima, Gail Mandel, and Joseph R Fetcho. Distribution of prospective glutamatergic, glycinergic,
393 and GABAergic neurons in embryonic and larval zebrafish. *The Journal of comparative neurology*, 480(1):1–18,
394 November 2004.
- 395 [24] Amina Kinkhabwala, Michael Riley, Minoru Koyama, Joost Monen, Chie Satou, Yukiko Kimura, Shin-Ichi
396 Higashijima, and Joseph Fetcho. A structural and functional ground plan for neurons in the hindbrain of zebrafish.
397 *Proceedings of the National Academy of Sciences of the United States of America*, 108(3):1164–1169, January
398 2011.
- 399 [25] Minoru Koyama, Amina Kinkhabwala, Chie Satou, Shin-Ichi Higashijima, and Joseph Fetcho. Mapping a
400 sensory-motor network onto a structural and functional ground plan in the hindbrain. *Proceedings of the Na-*
401 *tional Academy of Sciences of the United States of America*, 108(3):1170–1175, January 2011.
- 402 [26] R K Lee, R C Eaton, and S j Zottoli. Segmental arrangement of reticulospinal neurons in the goldfish hindbrain.
403 *The Journal of comparative neurology*, 329(4):539–556, March 1993.
- 404 [27] Yukiko Kimura, Yasushi Okamura, and Shin-Ichi Higashijima. alx, a zebrafish homolog of Chx10, marks ip-
405 silateral descending excitatory interneurons that participate in the regulation of spinal locomotor circuits. *The
406 Journal of neuroscience : the official journal of the Society for Neuroscience*, 26(21):5684–5697, May 2006.
- 407 [28] Alicia Colombo, Germán Reig, Marina Mione, and Miguel L Concha. Zebrafish BarH-like genes define discrete
408 neural domains in the early embryo. *Gene Expression Patterns*, 6(4):347–352, April 2006.
- 409 [29] Shaista Jabeen and Vatsala Thirumalai. Distribution of the gap junction protein connexin 35 in the central nervous
410 system of developing zebrafish larvae. *Frontiers in Neural Circuits*, 7:91, 2013.
- 411 [30] D W Caley and A B Butler. Formation of central and peripheral myelin sheaths in the rat: an electron microscopic
412 study. *The American journal of anatomy*, 140(3):339–347, July 1974.
- 413 [31] J Rosenbluth and S L Palay. The fine structure of nerve cell bodies and their myelin sheaths in the eighth nerve
414 ganglion of the goldfish. *The Journal of biophysical and . . .*, 1961.
- 415 [32] Michael J F Barresi, Lara D Hutson, Chi-Bin Chien, and Rolf O Karlstrom. Hedgehog regulated Slit expression
416 determines commissure and glial cell position in the zebrafish forebrain. *Development (Cambridge, England)*,
417 132(16):3643–3656, August 2005.
- 418 [33] Ronald S Petralia, Ya-Xian Wang, Mark P Mattson, and Pamela J Yao. Structure, Distribution, and Function of
419 Neuronal/Synaptic Spinules and Related Invaginating Projections. *NeuroMolecular Medicine*, 17(3):211–240,
420 May 2015.
- 421 [34] Alicia Guemez-Gamboa, Nicole G Coufal, and Joseph G Gleeson. Primary cilia in the developing and mature
422 brain. *Neuron*, 82(3):511–521, May 2014.
- 423 [35] Mati Joshua, Javier F Medina, and Stephen G Lisberger. Diversity of Neural Responses in the Brainstem during
424 Smooth Pursuit Eye Movements Constrains the Circuit Mechanisms of Neural Integration. *The journal of
425 neuroscience*, 33(15):6633–6647, April 2013.
- 426 [36] Emre Aksay, Itsaso Olasagasti, Brett D Mensh, Robert Baker, Mark S Goldman, and David W Tank. Functional
427 dissection of circuitry in a neural integrator. *Nature neuroscience*, 10(4):494–504, April 2007.
- 428 [37] Owen Debowy and Robert Baker. Encoding of eye position in the goldfish horizontal oculomotor neural integra-
429 tor. *Journal of Neurophysiology*, 105(2):896–909, February 2011.

- 430 [38] Emre Aksay, Robert Baker, H Sebastian Seung, and David W Tank. Correlated discharge among cell pairs within
431 the oculomotor horizontal velocity-to-position integrator. *The Journal of neuroscience : the official journal of*
432 *the Society for Neuroscience*, 23(34):10852–10858, November 2003.
- 433 [39] Juan Carlos Tapia, Narayanan Kasthuri, Kenneth J Hayworth, Richard Schalek, Jeff W Lichtman, Stephen J
434 Smith, and JoAnn Buchanan. High-contrast en bloc staining of neuronal tissue for field emission scanning
435 electron microscopy. *Nature Protocols*, 7(2):193–206, February 2012.
- 436 [40] Kenneth J Hayworth, Josh L Morgan, Richard Schalek, Daniel R Berger, David G C Hildebrand, and Jeff W
437 Lichtman. Imaging ATUM ultrathin section libraries with WaferMapper: a multi-scale approach to EM recon-
438 struction of neural circuits. *Frontiers in Neural Circuits*, 8:68, 2014.
- 439 [41] Narayanan Kasthuri, Kenneth Jeffrey Hayworth, Daniel Raimund Berger, Richard Lee Schalek, José Angel
440 Conchello, Seymour Knowles-Barley, Dongil Lee, Amelio Vázquez-Reina, Verena Kaynig, Thouis Raymond
441 Jones, Mike Roberts, Josh Lyskowski Morgan, Juan Carlos Tapia, H Sebastian Seung, William Gray Ron-
442 cal, Joshua Tzvi Vogelstein, Randal Burns, Daniel Lewis Sussman, Carey Eldin Priebe, Hanspeter Pfister, and
443 Jeff William Lichtman. Saturated Reconstruction of a Volume of Neocortex. *Cell*, 162(3):648–661, July 2015.
- 444 [42] Albert Cardona, Stephan Saalfeld, Johannes Schindelin, Ignacio Arganda-Carreras, Stephan Preibisch, Mark
445 Longair, Pavel Tomancak, Volker Hartenstein, and Rodney J Douglas. TrakEM2 software for neural circuit
446 reconstruction. *PLoS ONE*, 7(6):e38011, 2012.
- 447 [43] Andrew Miri, Kayvon Daie, Aristides B Arrenberg, Herwig Baier, Emre Aksay, and David W Tank. Spatial
448 gradients and multidimensional dynamics in a neural integrator circuit. *Nature neuroscience*, 14(9):1150–1159,
449 September 2011.
- 450 [44] Kayvon Daie, Mark S Goldman, and Emre R F Aksay. Spatial patterns of persistent neural activity vary with the
451 behavioral context of short-term memory. *Neuron*, 85(4):847–860, February 2015.

452 **8 Figure legends**

453 **Figure1: Functional and structural imaging of integrator neurons.**

454 (A) (a) Top - Larval zebrafish schematic showing the region where functional imaging was performed (black box)
455 located in the hindbrain, along with recording of eye-tracking behavior.
456 Bottom - A single imaging plane showing neurons loaded with calcium indicator OGB-1. Identified integrator neurons
457 are show in colored circles. Colors reflect the level of persistence of the neuron. Scale bar $20\mu m$
458 (b) Spontaneous eye movement (top, blue line) showing saccades (sharp vertical lines) and post-saccadic fixations
459 (horizontal lines). Ipsilateral saccades are indicated by black arrows. Colored traces below are the changes in fluores-
460 cence from individual neurons in (a). Colors represent the persistence level of the neuron.
461 (c) Normalized fluorescence and firing rate of neurons in (a). Thick line shows the average, with shaded region show-
462 ing the SEM. Dotted line is the exponential fit to determine persistence time constant, represented as $\log(\tau)$.
463 (B) Serial-sections for electron microscopy were collected on tape in an automated manner. Each section was imaged
464 at low-resolution (b1). A region-of-interest that corresponded with the functionally imaged area was defined (black
465 box in b1) for high-resolution imaging (b2). All such images were aligned to generate a 3D EM volume.
466 (C) Registration of LM volume to EM volume to locate the neurons that were involved in the behavior. Red arrows
467 indicate the same features in both LM and EM. Scale bar $20\mu m$
468 (D) An example EM plane showing anatomical landmarks, Mauthner neuron (black star), Mi2 (red stars), Mi3 (blue
469 stars) and Ca (green stars). Anatomical locations of all identified integrator neurons (colored circles) and all remaining
470 cell bodies in the imaged EM volume (‘●’ symbol). Colors of the integrator neurons correspond to the persistence
471 time of the neuron. Lower panel is a distribution of all neurons along the medio-lateral axis with integrator neurons
472 overlaid. Dotted lines (cyan) are the identified somata stripes S 1-3.

473 **Figure2: Ultrastructural features of Integrator neurons.**

474 (A) Integrator neuron with ipsilaterally projecting axon (dark lines) with presynaptic (green circles) and dendrites (light
475 lines) with postsynaptic (red circles) locations. Parts of the axon of this integrator neuron are loosely-myelinated. In-
476 sets shows axons with loose myelin (colored), arrows showing individual myelin sheaths. Open arrow head shows the
477 location of axon initiation.
478 (B) Integrator neuron with ipsilateral projecting axon. Axon is studded with presynaptic sites that are clustered along
479 neurite. Inset is a 3D reconstruction of axon termination zone with a large vesicle cloud (blue) with multiple post
480 synaptic densities (yellow) opposed to the vesicles. Numbers correspond to EM insets showing the synapses. M -
481 Mitochondria, V - Vesicles. Arrows show the synapses at those locations.
482 (C) Integrator neuron with contralateral projecting axon. Putative contralateral axon emerges from somata and is en-
483 gulped by glial before crossing the midline. (EM insets at numbered locations G - Glia, A - Axon) Open arrowhead
484 shows the axon initiation site.
485 (D) Integrator neurons with only contralaterally projecting axon. Putative axon is engulfed by glia before crossing the
486 midline,(EM insets at numbered locations G - Glia, A - Axon). Bottom EM panel shows primary cilium highlighted
487 with yellow arrow. Note all the integrator somata in this volume give rise to a cilium, but it is shown for this neuron.

489 **Figure3: Integrator neurons projection patterns and synaptic distribution.**

490 (A) Colored panels show three views of reconstructed integrator neurons, grouped according to their axonal projection
491 patterns. Left, 6 integrator neuron with ipsilateral projecting axons - ipsi-only group, pink background. Middle, 9
492 integrator neurons with midline crossing contralateral only putative-axon – contra-only, orange background. Right, 6,
493 integrator neurons with unknown axonal projection – unknown, blue background. Axons - dark line, dendrites - light
494 lines, red circles - postsynaptic sites, green circles - presynaptic sites.
495 (B) Box plot of the number of synapses in each group. Black line is the median ($p = 0.004$, significance reported as
496 Wilcoxon rank-sum test).
497 (C) Box plot of the Synaptic density for each group. Black lines are the medians.
498 (D) Normalized distribution of the synaptic pathlength. Red - postsynaptic sites, green - Presynaptic sites. Black
499 vertical lines, with adjoining colored numbers represent the means of the distribution.
500 (E) Box plots of the intersynaptic path length for all four groups. Open circles are outliers, not shown beyond $10\mu m$..
501 (F) Axonal and dendritic diameter of all neurons in each of the four groups. Grey dots are averages for each neuron
502 and black dots are averages per group. A - Axon, D - Dendrite.

504

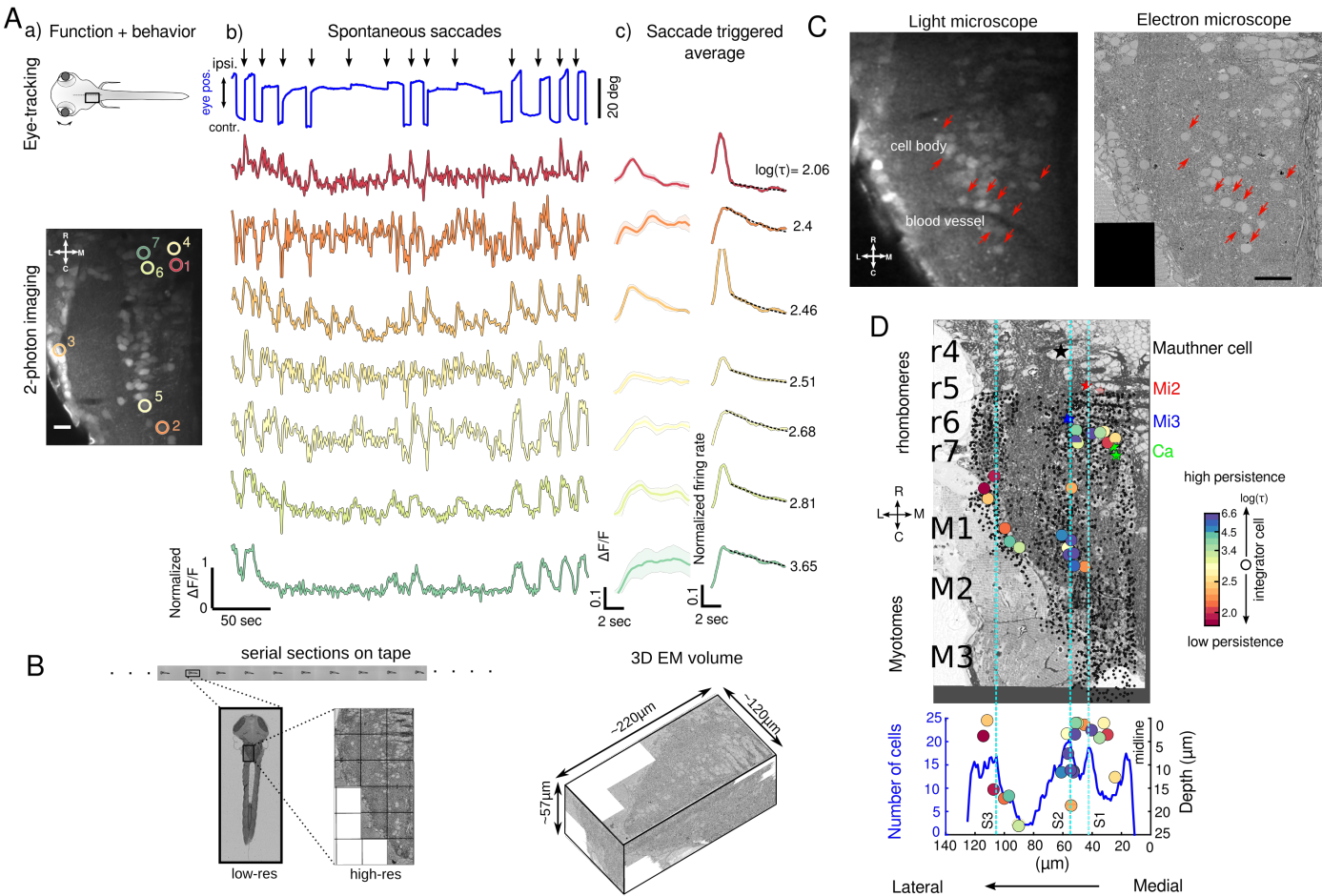


Figure 1:

505 Figure4: Integrator neurons are synaptically connected.

506 (A) Planar organization of ipsi (pink) and contra (orange) projecting neurons postsynaptic sites. Grid represents the
507 best fit plane through the cloud of points for each group.

508 (B) (Top) Stratification profile of all ipsi-only group of neurons. Two side views show the stratification of the dendrites,
509 presynaptic and postsynaptic sites along the dorso-ventral and medio-lateral axis. Dotted line represent the location of
510 the somatic peaks that was computed in Figure 1.

511 (Bottom) Stratification profile of all contra-only group of neurons.

512 (C) Three views of synaptically connected integrator neurons. Synapses from the ipsi-only group onto another neuron
513 from ipsi-only group are in top left (black circles) and onto contra-only neurons are at bottom right. Black dots repre-
514 sent the location of the synapses, with insets showing the electron micrograph at two representative locations, colors
515 in the inset are representative of the cells to which the synapses belong.

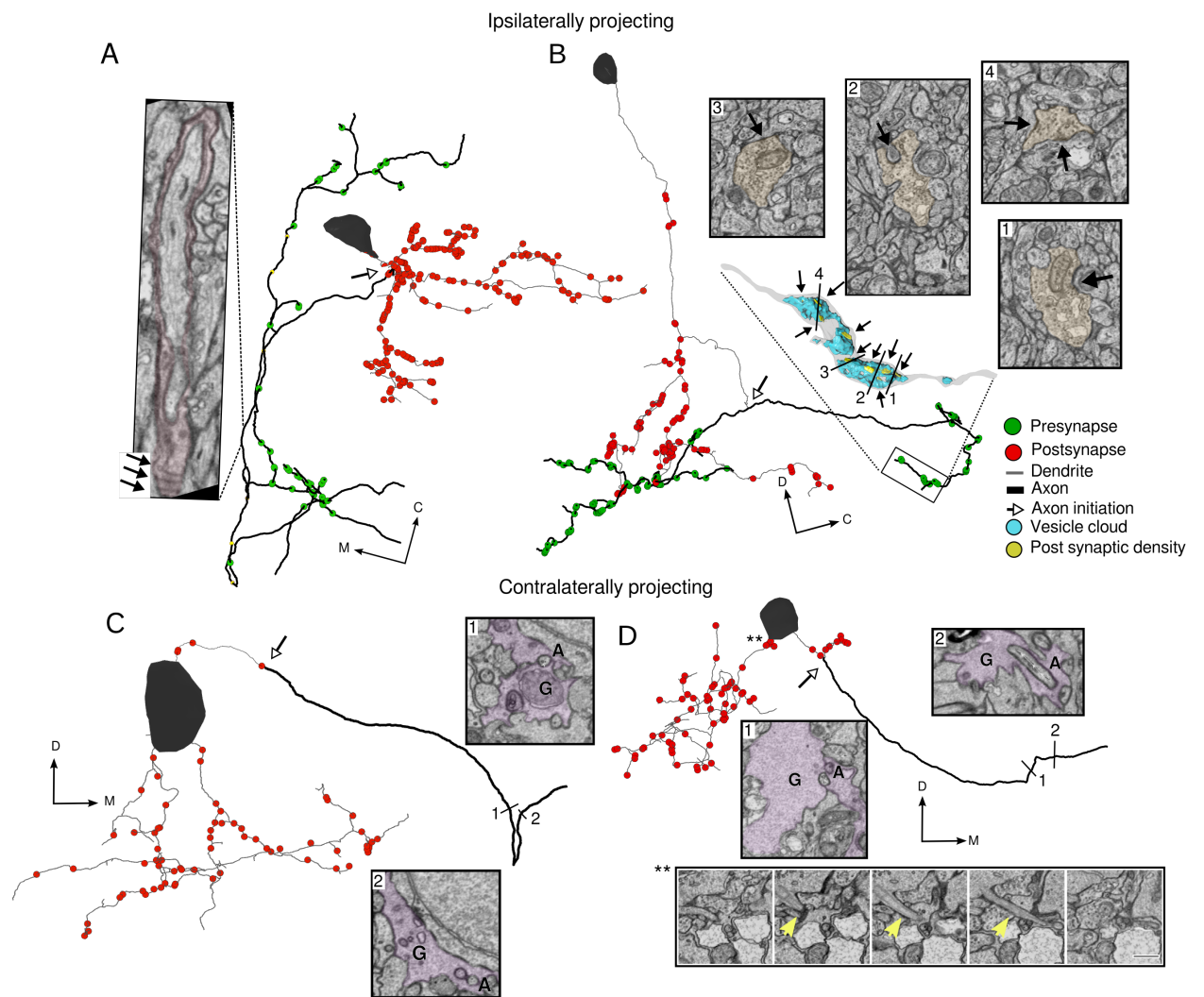
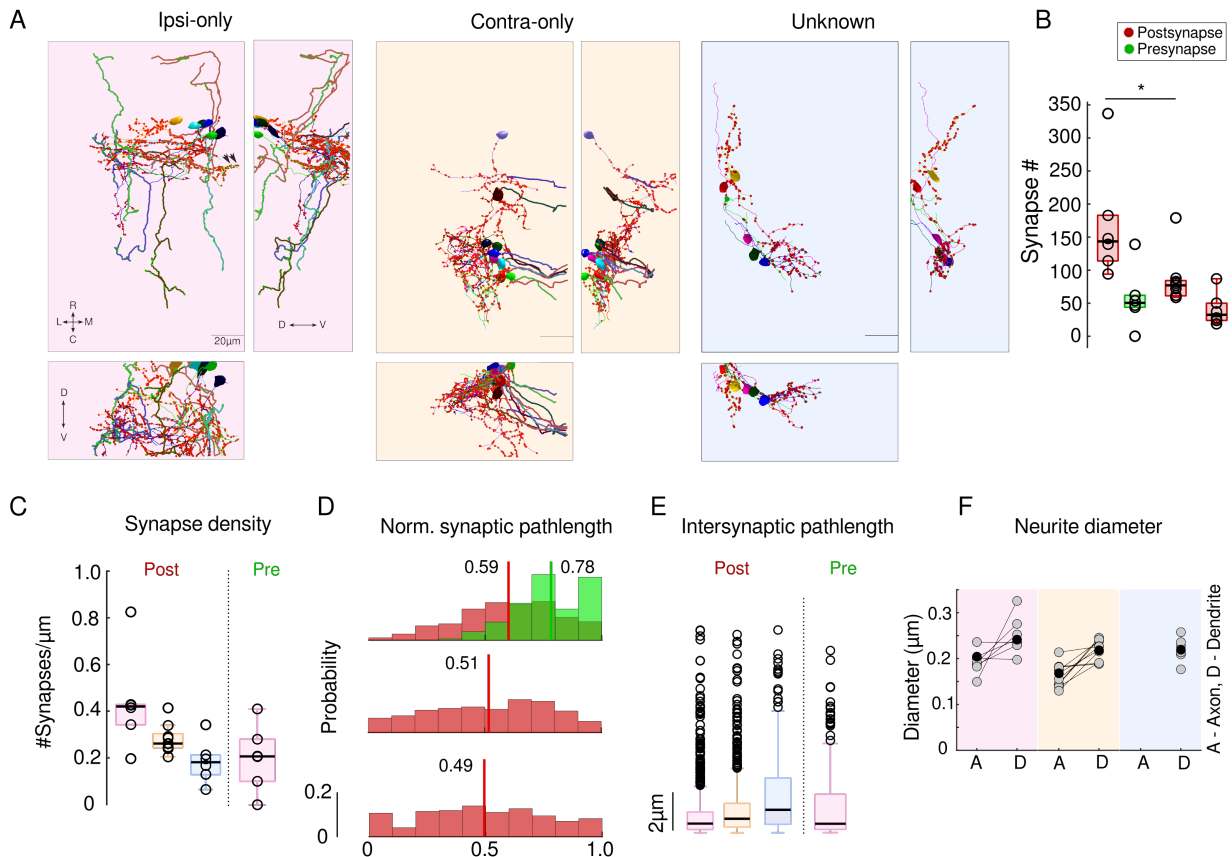


Figure 2:

Figure 3:



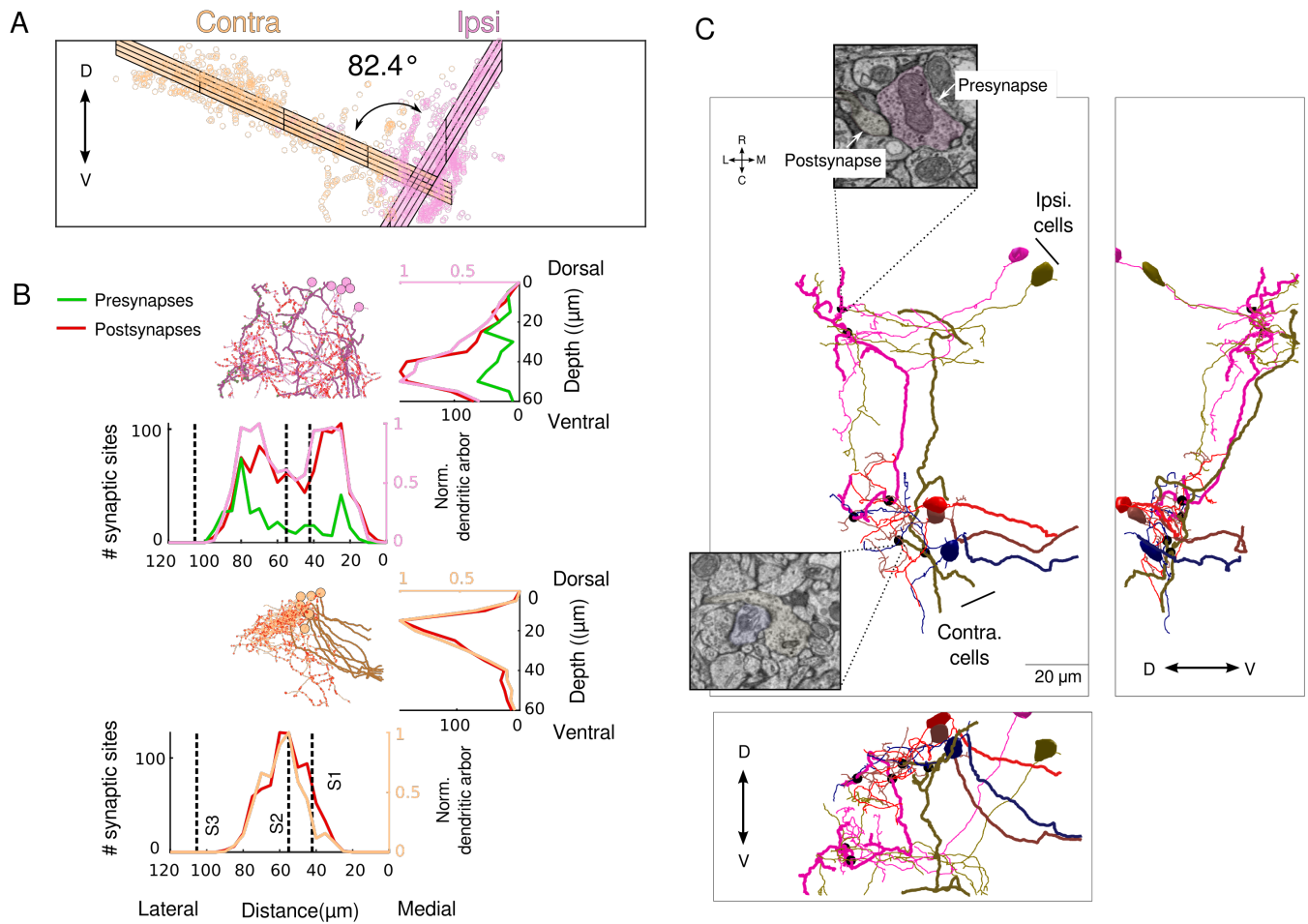


Figure 4: